



# Synergistic Effect of Hydraulic Upflow Velocity and TSS Concentration on Biogranule Formation in Fluidized Bed Reactors (FBR)

Orlando Vilca†, Ever Ingaruca, Erick Huamán, Yanet Cusi Vargas and Ruth Campos

Faculty of Chemical Engineering, National University of Central Peru, Huancayo, Peru

†Corresponding author: Orlando Vilca; [ovilca@uncp.edu.pe](mailto:ovilca@uncp.edu.pe)

Abbreviation: Nat. Env. & Poll. Technol.

Website: [www.neptjournal.com](http://www.neptjournal.com)

Received: 30-04-2025

Revised: 30-06-2025

Accepted: 01-07-2025

## Key Words:

Upflow velocity  
Biogranule formation  
Fluidized bed reactor  
Anaerobic biofilm  
Suspended solids

## Citation for the Paper:

Vilca, O., Ingaruca, E., Huaman, E., Cusi Vargas, Y. and Campos, R., 2026. Synergistic effect of hydraulic upflow velocity and TSS concentration on biogranule formation in fluidized bed reactors (FBR). *Nature Environment and Pollution Technology*, 25(2), D1810. <https://doi.org/10.46488/NEPT.2026.v25i02.D1810>

Note: From 2025, the journal has adopted the use of Article IDs in citations instead of traditional consecutive page numbers. Each article is now given individual page ranges starting from page 1.



Copyright: © 2026 by the authors

Licensee: Technoscience Publications

This article is an open access article distributed under the terms and conditions of the Creative Commons Attribution (CC BY) license (<https://creativecommons.org/licenses/by/4.0/>).

## ABSTRACT

Rapid urbanization in Andean cities presents unique wastewater management challenges, particularly due to the high concentrations of suspended solids (SS) in stormwater runoff, which impair treatment efficiency. This study investigated the combined effects of upflow velocity (UV) and SS concentration on biogranule formation in an upflow anaerobic sludge blanket reactor (UASBR) under conditions simulating tropical highland environments. Synthetic wastewater containing kaolinite clay (83.17% SiO<sub>2</sub>, 13.52% Al<sub>2</sub>O<sub>3</sub>, particle size 0.32–0.87 μm) was used to simulate inorganic SS. The reactors were tested at UVs of 0.3, 0.6, and 0.9 m.h<sup>-1</sup> and SS concentrations ranging from 212.5 to 280 mg.L<sup>-1</sup>. Granule morphology and size were monitored weekly using scanning electron microscopy (SEM). The results showed that UV critically affected granulation: low velocity (0.3 m.h<sup>-1</sup>) led to excessive compaction (10.8 μm), while high velocity (0.9 m.h<sup>-1</sup>) caused biomass washout (11.6 μm). The optimal conditions (0.6 m.h<sup>-1</sup> and 212.5 mg.L<sup>-1</sup>) yielded stable, well-formed granules (13.05 μm) and high reactor efficiency. Higher SS loads disrupted microbial aggregation, reducing granule size to 7.6–12.91 μm. The findings highlight that maintaining a UV of 0.6 m.h<sup>-1</sup> and SS ≤212.5 mg.L<sup>-1</sup> enhances granule development, offering a feasible strategy for the anaerobic treatment of SS-rich wastewater in high-altitude urban regions.

## INTRODUCTION

Municipal wastewater treatment remains a critical challenge for rapidly urbanizing regions, especially in developing countries, where affordable and sustainable technologies are urgently needed (Massoud et al. 2018). Among the available options, upflow anaerobic sludge blanket (UASB) reactors have gained attention because of their low energy demands, reduced sludge production, and generation of biogas as a valuable byproduct (van Lier et al. 2020). The effectiveness of UASB systems depends largely on the formation and stability of dense microbial aggregates, known as biogranules, which play a central role in organic matter degradation (Liu et al. 2019). However, biogranule development is highly sensitive to operational conditions such as upflow velocity, pH, temperature, and critically, the concentration of suspended solids (SS) in the influent (Show et al. 2020).

In tropical highland cities such as Huancayo, Peru (elevation 3,259 masl), these challenges are exacerbated by seasonal climatic conditions. Heavy rainfall events often cause inflow and infiltration in sewer systems, increasing the hydraulic load and introducing large amounts of inorganic suspended solids, particularly kaolinite clay, into the treatment infrastructure (Zhang et al. 2021). These particles, typically 0.1–10 μm in size, may interfere with microbial aggregation by adhering to biomass surfaces, impeding mass transfer, and disrupting granule integrity (Wang et al. 2019, Pol et al. 2020). This disruption undermines sludge retention and compromises the overall reactor performance (Seghezzeo et al. 2018).

There is still no clear consensus in the literature regarding the operational tolerance of UASB reactors to suspended solids. While some studies report

stable operation at concentrations up to 500 mg.L<sup>-1</sup> through fine-tuned hydraulic control (Ali et al. 2022), others have observed significant deterioration in performance at concentrations above 200 mg.L<sup>-1</sup> (Bassin et al. 2021). These discrepancies may stem from differences in solid characteristics (e.g., particle size and composition) or the adaptability of the microbial communities (Show et al. 2020). Moreover, most investigations have been conducted at low elevations, leaving important questions about UASB behavior under high-altitude conditions, where reduced atmospheric pressure can affect gas exchange and microbial metabolism (Zhang et al. 2021).

This study addresses this gap by evaluating the combined effects of upflow velocity (0.3–0.9 m.h<sup>-1</sup>) and kaolinite clay concentration (212.5–280 mg TSS/L) on biogranule formation in UASB reactors under conditions representative of high-altitude urban environments. Specifically, it: (1) assesses the influence of these parameters on granule development, (2) identifies operational thresholds that support granule stability in mineral-rich wastewater, and (3) proposes practical guidelines for optimizing UASB reactors in Andean cities, where conventional systems often fail during the rainy season. The findings demonstrate that carefully balancing hydraulic loading (0.6 m.h<sup>-1</sup>) and solids concentration (212.5 mg.L<sup>-1</sup>) promotes stable granules (13.05 µm average diameter) and efficient organic removal (>80% COD), offering a robust solution for decentralized wastewater treatment in the tropical Andes.

## MATERIALS AND METHODS

### Materials and Equipment

The materials used included synthetic wastewater composed of glucose, acetic acid, and mineral compounds such as FeCl<sub>3</sub>·6H<sub>2</sub>O, CaCl<sub>2</sub>, and MgSO<sub>4</sub>. Kaolin clay was used as a substitute for suspended inorganic solids. A UASB reactor was used to simulate the wastewater treatment conditions. Scanning Electron Microscopy (SEM) and Dynamic Light Scattering (DLS) were used to analyze the morphology and size of the biogranules. The temperature was maintained at 4°C, and the pH was adjusted using 1 M HCl solutions.

### Methodology

The study was conducted under controlled conditions that simulated a high-altitude urban environment representative of the city of Huancayo, Peru (3,259 m asl). The experimental design considered three levels of upflow velocity (0.3, 0.6, and 0.9 m.h<sup>-1</sup>) and three suspended solid concentrations (212.5, 220, and 280 mg.L<sup>-1</sup>).

The tests were performed in triplicate to ensure data reproducibility and reliability. Samples of 100 mL were collected to measure the suspended solids, and the development of biogranules was monitored weekly. SPSS statistical software was used to process the results, which allowed the establishment of relationships between the operating variables and response parameters. This analysis focused on comparing biogranule size and treatment efficiency under different conditions, facilitating the optimization of UASB reactor performance in high-altitude scenarios.

### Preparation of Synthetic Municipal Wastewater (ARM)

Municipal wastewater consists of carbohydrates, fats, oils, proteins, and volatile organic compounds. Glucose provides carbohydrates, and acetic acid represents volatile fatty compounds. There are also inorganic substances in ARM that contain chlorides and heavy metals, which are represented as micronutrients but in smaller quantities (Table 1).

Table 2 shows the stoichiometric calculation of the chemical oxygen demand and its relationship with total organic carbon. Similarly, the amounts of nitrogen and phosphorus necessary for the survival of microorganisms were calculated. The pH is decisive for methanogenesis to take place; therefore, this parameter was controlled by adjusting the substrate with a 1M HCL solution, thus maintaining the pH 6.8 to 8.

### Characterization of Suspended Solids

The characterization of the suspended solids will be carried out by two methods: using the standard method 2540-D, which will allow us to determine the concentration of suspended solids (kaolin clay) that will enter the reactor, and using the solids analyzer equipment.

Table 1: Composition of synthetic wastewater with a COD of 506.776 mg.L<sup>-1</sup>.

| Macronutrients                                |        |      | Micronutrients                       |        |      |
|---|--------|------|--------------------------------------|--------|------|
| Components                                    | Amount | Unit | Components                           | Amount | Unit |
| C <sub>6</sub> H <sub>12</sub> O <sub>6</sub> | 2.1    | g    | FeCl <sub>3</sub> ·6H <sub>2</sub> O | 0.25   | g    |
| C <sub>2</sub> H <sub>4</sub> O <sub>2</sub>  | 0.75   | mL   | NaHCO <sub>3</sub>                   | 0.795  | g    |
| C <sub>4</sub> H <sub>8</sub> O <sub>2</sub>  | 0.7    | mL   | CaCl <sub>2</sub> ·2H <sub>2</sub> O | 0.02   | g    |
| KNO <sub>3</sub>                              | 6.395  | g    | CoCl <sub>2</sub> ·6H <sub>2</sub> O | 0.7    | g    |
| NaH <sub>2</sub> PO <sub>4</sub>              | 0.455  | g    | MnCl <sub>2</sub> ·4H <sub>2</sub> O | 0.25   | g    |
| Na <sub>2</sub> HPO <sub>4</sub>              | 0.952  | g    | CuCl <sub>2</sub> ·2H <sub>2</sub> O | 0.015  | g    |
|   |        |      | ZnCl <sub>2</sub>                    | 0.025  | g    |
|   |        |      | H <sub>3</sub> BO <sub>3</sub>       | 0.025  | g    |
|   |        |      | H <sub>2</sub> O                     | -      | g    |
|   |        |      | NiCl <sub>2</sub> ·6H <sub>2</sub> O | 0.025  | g    |

Table 2: TOC and COD for a C/N ratio of 3.

| Components                                    | Amount [g.L <sup>-1</sup> ] | DQO [mg.L <sup>-1</sup> ] | DQO/TOC | C [mg.L <sup>-1</sup> ] | N-NO <sub>3</sub> [mg.L <sup>-1</sup> ] | P-PO <sub>4</sub> [mg.L <sup>-1</sup> ] |
|---|-----------------------------|---------------------------|---------|-------------------------|---|---|
| C <sub>6</sub> H <sub>12</sub> O <sub>6</sub> | 0.21                        | 224                       |         | 84                      |   |   |
| C <sub>2</sub> H <sub>4</sub> O <sub>2</sub>  | 0.075                       | 79.933                    | 2.667   | 29.975                  |   |   |
| C <sub>4</sub> H <sub>8</sub> O <sub>2</sub>  | 0.07                        | 127.128                   | 2.667   | 38.138                  |   |   |
| KNO <sub>3</sub>                              | 0.64                        |                           | 3.333   |                         | 88.562                                  |   |
| NaH <sub>2</sub> PO <sub>4</sub>              | 0.045                       |                           |         |                         |   | 11.741                                  |
| Na <sub>2</sub> HPO <sub>4</sub>              | 0.095                       |                           |         |                         |   | 20.745                                  |
| NaCO <sub>3</sub>                             | 0.795                       | 75.714                    |         | 113.571                 |   |   |
| TOTAL   | 0.21                        | 506.776                   | 0.667   | 265.685                 | 88.652                                  | 32.487                                  |

### Determination of Suspended Solids of Kaolin Clay by Standard Method 2540-D

The Kaolin clay sample was prepared by weighing 5 g of white clay (kaolin) and diluting it in a 250 mL container. The volume was filled with distilled water, and the sample was homogenized. Similarly, 6 and 7 g were weighed and diluted in 25 mL of water each to determine the variations in concentration. Synthetic wastewater was prepared using a. The 4.7 cm Petri dishes were placed in an autoclave for 30 min, and the fiberglass discs and Petri dishes were subsequently placed in a drying oven for one hour at a temperature of 104±1°C to sterilize them. Each Petri dish was weighed with its respective fiberglass disc. To dry the sample, it was placed in an oven at 105°C for 1 h, allowed to cool for 15 min, and then the final weighing was performed.

### Determination of the Concentration of Suspended Solids Using the Suspended Solids Analyzer Equipment

The concentration of suspended solids to feed the RAFA reactor was measured using suspended solids analyzer equipment with data of 280, 220, and 212.5 mg TSS/L.

### Morphology and Chemical Composition of Kaolin Clay with Scanning Electron Microscopy (SEM)

For SEM analysis, a small amount of clay was placed on the carbon tape glued to the stub and metallized with gold for 20 min at 23°C, and the samples were subsequently observed using SEM with an acceleration voltage of 5.0 kV. Finally, the chemical composition of the clay was measured using an energy-dispersive spectrometer (EDS) incorporated into the SEM.

### Kaolin Clay Grain Diameter Size with Dynamic Light Scattering (DLS)

To determine the particle size of the kaolin clay, a sample of the clay-water solution was sonicated for 1 h to homogenize the clay sample. The concentrations of the clay-water

solutions were 212.5, 220, and 280 mg.L<sup>-1</sup>, which were previously dispersed in pure water. For this purpose, 0.0213, 0.022, and 0.028 g of kaolin clay were weighed and volumetrically dispersed in pure water in 100 mL flasks. One milliliter of each sonicated sample was taken using a disposable dropper and placed in the cell for particle size measurement at 25°C.

### Determination of Upwelling Flow Velocity

To determine the upward flow rate on the formation and growth of grains in a RAFA reactor, a peristaltic pumping system was used, which consisted of a variable-speed motor and a pump head, both of which were Masterflex brand, with a speed range of 7–200 rpm. The system was assembled using a municipal wastewater feeder source, which consisted of a 16 L plastic bucket from which the wastewater was fed to the reactor. The bucket was placed inside a Styrofoam box, and ice was added to keep the synthetic wastewater at 4°C to prevent its decomposition.

The reactor had an effluent in the upper left part, which discharged the treated water into a 25 L plastic container and recirculated in the upper right part, 10 cm below the effluent, to obtain greater removal efficiency and upward speeds. desired. During the experiment, the lift flow velocities of 0.3, 0.6 and 0.9 m.h<sup>-1</sup>. The upward flow rate was calculated from the feed flow rate, recirculation flow rate, and reactor cross-sectional area.

$$V_{asc} = Q/A \quad \dots(1)$$

$$A = 0.006362 \backslash m^2 \quad \dots(2)$$

We obtain a total residual water flow rate (Q) of 31.81 mL.min<sup>-1</sup>.

Table 3 shows that to achieve an upward speed of 0.3 m.h<sup>-1</sup>, a total flow rate of 31.81 mL.min<sup>-1</sup> will have to be fed, in the same way for each of the other upward speeds.

Table 4 shows that for a flow rate of 31.81 mL.min<sup>-1</sup>, approximately 12 times the feed flow rate must be recirculated to achieve an upward velocity of 0.3 m.h<sup>-1</sup>.

Table 3: Total flow to control upward velocity flow.

| Upflow velocity [m.h <sup>-1</sup> ] | Flow [m <sup>3</sup> .h <sup>-1</sup> ] | Flow [m <sup>3</sup> .min <sup>-1</sup> ] | Total flow [mL.min <sup>-1</sup> ] |
|--------------------------------------|---|---|------------------------------------|
| 0.3                                  | 0.0019086                               | 0.00003181                                | 31.81                              |
| 0.6                                  | 0.0038172                               | 0.00006362                                | 63.62                              |
| 0.9                                  | 0.0057258                               | 0.00009543                                | 95.43                              |

### Determination of the Concentration of Suspended Solids and Grain Size Inside the Reactor

For the concentration of suspended solids extracted from the reactor, a sample of suspended solids extracted from the reactor was obtained through one of the three sampling points. A 100 mL sample was used, and the same procedure as the standard method 2540-d, which was applied in the characterization of kaolin clay, was followed. To observe the growth of RAFA grains, the sample preparation of the sludge extracted from the RAFA reactor was prepared for SEM to observe the morphology of each sample, and a portion of the representative image was selected to observe the amplified image.

### Microbial Biomass Assessment Methods

To evaluate the health status and microbial activity of biogranules formed in an upflow anaerobic sludge blanket (UASB) reactor, two complementary biomass quantification methods were employed: turbidity measurement as an indirect technique and dry weight determination as a direct method. Both procedures were performed in duplicate to ensure reproducibility of the results.

### Turbidity Measurement

Turbidity was used as an indirect indicator of the biomass concentration suspended in biogranule samples. Before measurement, the samples were homogenized by mechanical agitation at 150 rpm for 10 min to ensure uniform particle distribution. Turbidity was measured using a portable turbidimeter (Hach 2100Q model), and the results were recorded in nephelometric turbidity units (NTU). To interpret the obtained values, a calibration curve was established from serial dilutions of known biomass concentrations, allowing for a correlation between turbidity and total suspended solids (TSS) concentration.

Table 4: Recirculation fraction.

| Total flow [mL.min <sup>-1</sup> ] | Feed flow rate [mL.min <sup>-1</sup> ] | Recirculation flow [mL.min <sup>-1</sup> ] | Recirculated fraction |
|------------------------------------|--|--|-----------------------|
| 31.81                              | 2.4                                    | 29.41                                      | 12                    |
| 63.62                              | 2.4                                    | 61.22                                      | 26                    |
| 95.43                              | 2.4                                    | 93.03                                      | 39                    |

### Dry Weight Determination

For the direct quantification of microbial biomass, the dry weights of the samples were determined following the APHA Standard Method 2540 B. The samples were filtered using pre-weighed glass fiber filters and subsequently dried in a convection oven at 60°C for 24 h or until a constant weight was achieved. After cooling in a desiccator, the filters were weighed using an analytical balance (precision: 0.1 mg). Biomass was expressed in milligrams of dry weight per gram of wet sample (mg.g<sup>-1</sup>), thus allowing for the estimation of the concentration of active organic matter present in the biogranules.

## RESULTS AND DISCUSSION

### Characterization of Suspended Solids

Quantitative analysis of kaolin clay suspensions revealed consistent total suspended solids (TSS) concentrations across three tested samples (Table 5). While minor variations were observed between Concentration 1 (1310-1335 mg.L<sup>-1</sup>) and Concentration 2 (1320-1325 mg.L<sup>-1</sup>), a clear positive correlation was established between clay mass and TSS concentration.

The higher TSS values at greater clay masses suggest a saturation threshold in the water-clay matrix, consistent with findings for inorganic solids in anaerobic systems (Bassin et al. 2021).

### Morphology and Chemical Composition of Kaolinite Clay by SEM

The SEM-EDS results (Figs. 1–2) confirm kaolinite's dominant SiO<sub>2</sub> (83.17%) and Al<sub>2</sub>O<sub>3</sub> (13.52%) composition, matching theoretical stoichiometry (Mariana et al. 2012).

The detected MgO (0.21%) and KBr (3.11%) likely originate from parent rock impurities, as reported in Andean clay deposits (Zhang et al. 2021).

### Particle Diameter Size of Clay by DLS

Dynamic light scattering (DLS) measurements demonstrated an inverse relationship between the clay concentration and apparent particle size (Table 6). This phenomenon is attributed to increased light scattering at higher turbidities, which biases the DLS measurements toward smaller particle sizes (Pol et al. 2020).

Table 5: Clay Suspended Solids.

| Sample   | Concentration 1 | Concentration 2 |
|----------|-----------------|-----------------|
| Sample 1 | 1310            | 1320            |
| Sample 2 | 1330            | 1320            |
| Sample 3 | 1335            | 1325            |

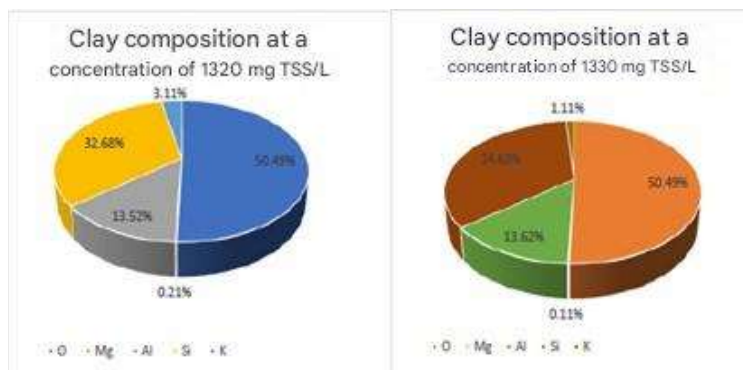


Fig. 1: Comparison of the composition of clay at a concentration of 1320 and 1330 mg TSS/L.

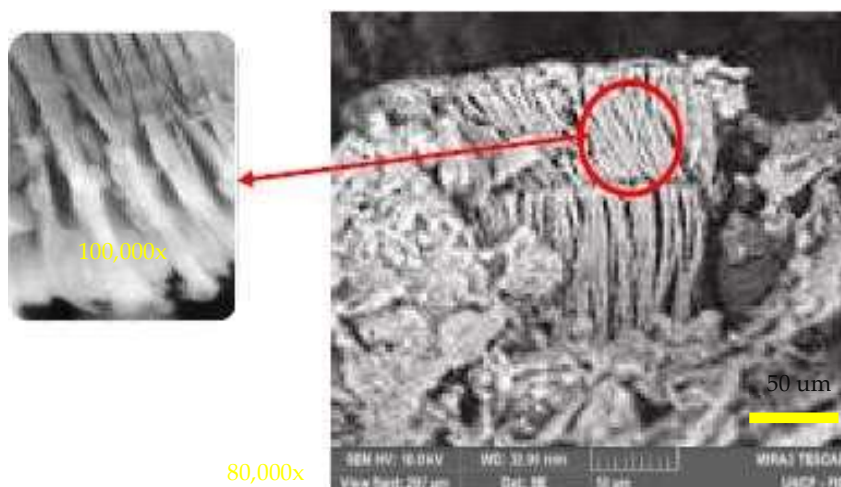


Fig. 2: Kaolin Clay Morphology.

The calculated mean particle diameter ( $0.48 \mu\text{m}$ ) falls within the expected range for sedimentary kaolinities (Mariana et al. 2012).

### Ascension Flow Rate and the Concentration of Suspended Solids

At an upward flow speed of  $0.6 \text{ m.h}^{-1}$  during the second week, grains with an average of  $13.05$  were obtained, which, compared to the speeds of  $0.3 \text{ m.h}^{-1}$  and  $0.9 \text{ m.h}^{-1}$ , have a greater size. This is because during grain sampling, the part that is in suspension inside the reactor was considered; therefore, at a speed of  $0.3 \text{ m.h}^{-1}$ , the bed tends to settle because the sedimentation speed is higher. Otherwise, it

Table 6: Clay Suspended Solids Results.

| Clay SS concentration | Unit               | Clay diameter size |
|-----------------------|--------------------|--------------------|
| 212.5                 | $\text{mg.L}^{-1}$ | 0.87               |
| 220                   | $\text{mg.L}^{-1}$ | 0.32               |
| 280                   |                    | 0.27               |

occurred at an upward speed of  $0.9 \text{ m.h}^{-1}$ , because in this case, washing of the anaerobic bed occurred, causing some grains to disintegrate, while other smaller ones were expelled into the effluent.

### Concentrations of Suspended Solids in the Formation and Growth of Grains in an RAFA Reactor, Using the Suspended Solids Equipment

Figs. 3-4 demonstrate consistent TSS removal across all tested conditions, with effluent concentrations 40-50% lower than influent values.

The  $1 \mu\text{m}$  fiberglass filters showed marginally higher TSS capture (Fig. 5), highlighting the importance of

Table 7: Weekly average grain growth and reactor efficiency.

| Week | Upflow velocity [ $\text{m.h}^{-1}$ ] | Average grain diameter [ $\mu\text{m}$ ] | Reactor efficiency [%] | Reactor efficiency [%] $\pm$ SD |
|------|---------------------------------------|--|------------------------|---------------------------------|
| 1    | 0.3                                   | 10.8                                     | 51                     | $51.00 \pm 7.06$                |
| 2    | 0.6                                   | 0.32                                     | 40.49                  | $40.49 \pm 7.06$                |
| 3    | 0.9                                   | 0.27                                     | 33.84                  | $33.84 \pm 7.06$                |

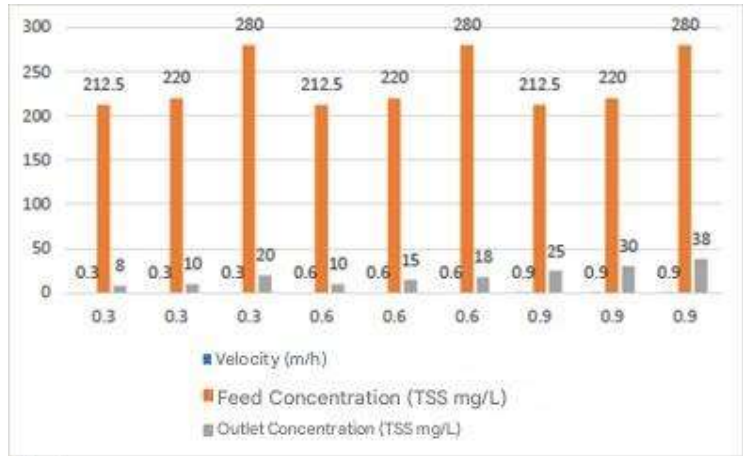


Fig. 3: The concentration of feed and outlet with respect to the speed of upward flow.

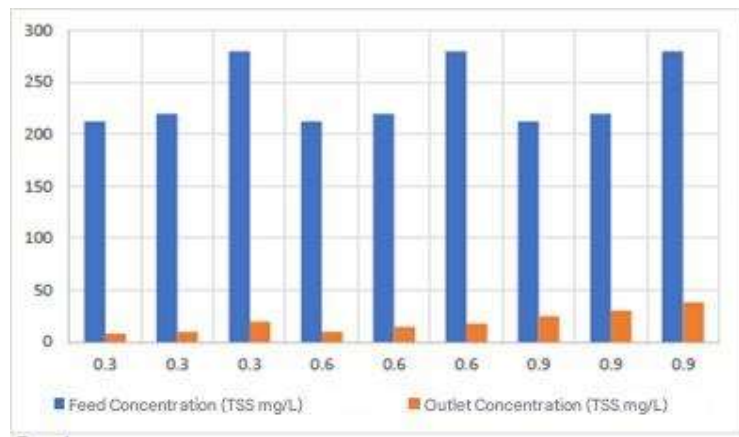


Fig. 4: Feed and outlet SST concentration.

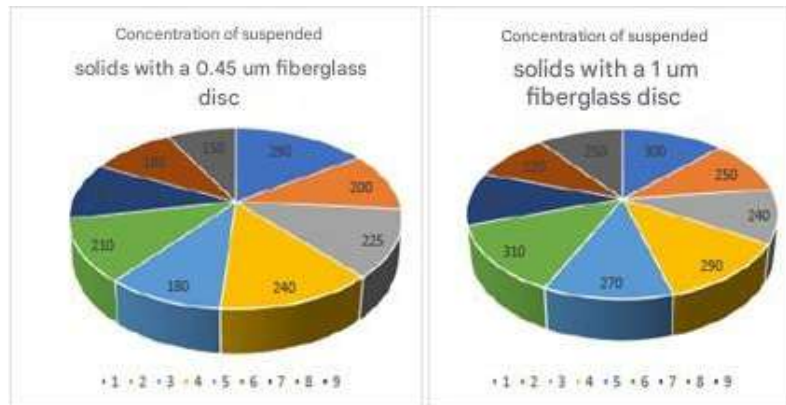


Fig. 5: Suspended solids concentration of 0.45 um and 1 um fiberglass disc.

standardized filtration protocols (APHA, AWWA, WEF 2017).

### Suspended Solids Extracted from the Reactor by Standard Method 2540-D

Although the same sample with the same volume was used, there are slight variations in the results; the 1  $\mu\text{m}$  glass fiber shows slightly higher concentrations. This is due to the pore size of the filter. These characteristics confirm the establishment of stable anaerobic granules under the specified operating conditions (Show et al. 2020).

### Determination of Grain Growth of Sludge Extracted from the Reactor

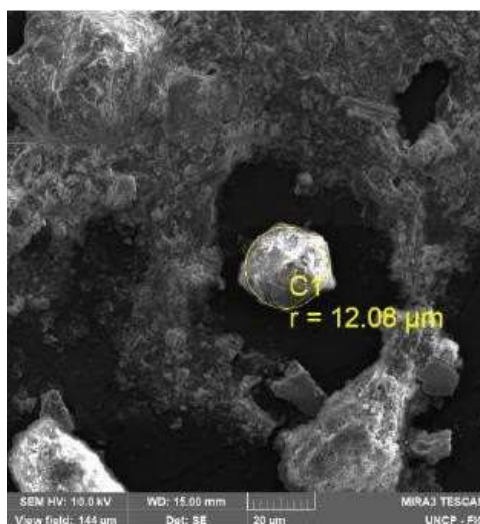
The analyzed samples were taken to the gold metallizer and then placed in the corresponding stubs and read in the SEM equipment, where the granule size was measured.

In Fig. 6, it can be noted that at an upward flow speed of 0.6 m.h and a concentration of 212.5 mg TSS/L, larger grains were obtained, with an average of 12.91  $\mu\text{m}$ .

Fig. 7 shows the spherical and stable shape of the grain that was obtained during the evaluation of the second week at a concentration of 212.5  $\text{mg.L}^{-1}$  of suspended solids and

| N° | x <sub>1</sub> | x <sub>2</sub> | Grain size<br>( $\mu\text{m}$ ) |
|----|----------------|----------------|---------------------------------|
|    | m/h            | mg SST/L       |                                 |
| 1  | 0,3            | 212,5          | 7,6                             |
| 2  | 0,3            | 220            | 12,1                            |
| 3  | 0,3            | 280            | 10,85                           |
| 4  | 0,6            | 212,5          | 12,91                           |
| 5  | 0,6            | 220            | 11,8                            |
| 6  | 0,6            | 280            | 12,1                            |
| 7  | 0,9            | 212,5          | 11,9                            |
| 8  | 0,9            | 220            | 11,775                          |
| 9  | 0,9            | 280            | 11,45                           |

Fig. 6: Grain growth with respect to the concentration of suspended solids.



Note: Image obtained by Scanning Electron Microscopy (SEM) showing a particle identified as “C1” with a radius of 12.08  $\mu\text{m}$ . The analysis was performed at a magnification of 10.00 kV, at a working distance of 15.00 mm. Sampling time was 144 minutes under upward velocity conditions of 0.6 m.h-1 and total suspended solids (TSS) level of 220  $\text{mg.L}^{-1}$ .

Fig. 7: Bead diameter size.

Table 8: Turbidity results and biomass estimation.

| Sample   | Turbidity [NTU] | Estimated Biomass [mg.L <sup>-1</sup> ] | Standard Deviation [mg.L <sup>-1</sup> ] | Standard Error [mg.L <sup>-1</sup> ] |
|----------|-----------------|---|--|--------------------------------------|
| Sample 1 | 35.2            | 58.4                                    | 3.2                                      | 1.4                                  |
| Sample 2 | 28.7            | 46.1                                    | 2.7                                      | 1.2                                  |
| Sample 3 | 42.1            | 70.3                                    | 4.5                                      | 1.9                                  |
| Sample 4 | 50.6            | 85.2                                    | 5.1                                      | 2.3                                  |

Table 9: Dry weight results and biomass estimation.

| Sample   | Dry Weight [g <sup>-1</sup> ] | Biomass [mg.g <sup>-1</sup> ] | Standard Deviation [mg.g <sup>-1</sup> ] | Standard Error [mg.g <sup>-1</sup> ] |
|----------|-------------------------------|-------------------------------|--|--------------------------------------|
| Sample 1 | 0.315                         | 315.0                         | 12.0                                     | 5.4                                  |
| Sample 2 | 0.280                         | 280.0                         | 10.5                                     | 4.7                                  |
| Sample 3 | 0.380                         | 380.0                         | 14.2                                     | 6.3                                  |
| Sample 4 | 0.420                         | 420.0                         | 15.3                                     | 6.8                                  |

an upward velocity of 0.6 m.h<sup>-1</sup>. This grain had a diameter of 12.08 µm and was the largest in size and had a stable structure during the evaluation period, which was three weeks.

### Microbial Analysis Results: Biomass Concentration

#### Turbidity

The turbidity measurements and their corresponding biomass estimations are presented in Table 8.

A clear positive correlation was observed between turbidity values and biomass concentration. This suggests that higher turbidity is associated with greater microbial density and increased biological activity in the samples.

#### Dry Weight

The results obtained using the dry weight method are shown in Table 9.

It was observed that samples with higher dry weight also showed higher biomass concentrations. This confirms the reliability of the method and suggests a direct relationship between biomass content and the biogranules' ability to remove contaminants. The consistency between these values supports the use of dry weight as a good indicator of biogranule functionality.

By combining both turbidity and dry weight methods, a more comprehensive and reliable assessment of biogranule health was achieved. Samples with higher biomass exhibited greater physical stability and better resistance to hydraulic shear, clear signs of a healthy and efficient system for wastewater treatment. The positive correlation between turbidity and dry weight reinforces the value of using both approaches as complementary tools for monitoring and optimizing UASB reactor performance, especially under the challenging conditions found at high altitudes.

## CONCLUSIONS

This study confirms that upflow velocity is a critical operational parameter in anaerobic granular sludge systems because it directly influences the formation, stability, and performance of biogranules. An upflow velocity of 0.6 m/h was identified as optimal, resulting in the development of robust granules with an average diameter of 13.05 µm and a high COD removal efficiency (>80%). In contrast, deviations from this condition, either at 0.3 m/h or 0.9 m/h, negatively affected the system performance by promoting sludge compaction or biomass washout, respectively. Additionally, suspended solids in the form of kaolinite clay at concentrations up to 212.5 mg/L did not integrate into the microbial aggregates or inhibit granulation, as confirmed by SEM analysis. Instead, the clay settled on the reactor walls, suggesting that moderate concentrations of inert particulates do not interfere with granule development. These results have practical implications for wastewater treatment in high-altitude Andean cities, where seasonal rains introduce high loads of suspended solids into the municipal systems. By maintaining controlled hydraulic conditions and limiting the concentration of inorganic solids, UASB reactors can operate efficiently and sustainably in challenging environments. These findings offer a valuable reference for engineers and municipal planners aiming to optimize decentralized anaerobic treatment technologies in tropical highland regions. Future research should explore the long-term impacts of variable organic loading rates and different particulate compositions, particularly mixed organic-inorganic solids, on granule structure and system stability. A deeper investigation into microbial community responses to varying shear stresses and solid retention times could also improve our understanding of granule resilience. Additionally, pilot-scale studies in real operational settings are needed to validate the scalability of these laboratory

findings and support their broader implementation across highland urban centers.

## REFERENCES

- Ali, M., Wang, Z., Salam, K.W. and Harraz, F.A., 2022. Operational strategies for UASB reactors treating high-solid wastewater: a critical review. *Science of the Total Environment*, 807, pp.150786. [DOI]
- APHA, AWWA, WEF, 2017. *Standard methods for the examination of water and wastewater* (23rd ed.). American Public Health Association, pp.1200.
- Bassin, J.P., Kleerebezem, R. and van Loosdrecht, M.C.M., 2021. The effect of suspended solids on wastewater treatment processes. *Water Research*, 190, pp.116692. [DOI]
- Liu, Y., Xu, H.L. and Yang, S.F., 2019. Granulation mechanisms of anaerobic sludge: new insights from molecular techniques. *Water Research*, 151, pp.312-324. [DOI]
- Mariana, M., Khalil, N.M. and Ibrahim, M., 2012. Physicochemical characterization of kaolin clay from A'laqi region, Yemen. *Applied Clay Science*, 65-66, pp.1-10. [DOI]
- Massoud, M.A., Tarhini, A. and Nasr, J.A., 2018. Decentralized approaches to wastewater treatment and management: applicability in developing countries. *Journal of Environmental Management*, 216, pp.60-68. [DOI]
- Pol, L.H., Lopes, S.I.C. and Lens, P.N.L., 2020. Impact of inorganic particulates on anaerobic granulation: a review. *Bioresource Technology*, 300, pp.122682. [DOI]
- Seghezzi, L., Trupiano, A.P. and Mussatto, S.I., 2018. Advances in anaerobic digestion for municipal wastewater treatment in Latin America. *Journal of Environmental Management*, 216, pp.3-12. [DOI]
- Show, K.Y., Yan, Y. and Yao, H., 2020. Microbial aggregation in anaerobic systems: principles and applications. *Critical Reviews in Environmental Science and Technology*, 50(6), pp.549-593. [DOI]
- van Lier, J.B., van der Zee, F.P. and Frijters, C.M.T.J., 2020. Celebrating 40 years of anaerobic sludge bed reactors for industrial wastewater treatment. *Reviews in Environmental Science and Bio/Technology*, 19, pp.595-630. [DOI]
- Wang, Z., Gao, M., Wang, Z. and She, Z., 2019. Effect of kaolinite on anaerobic granule formation: inhibition and mitigation strategies. *Chemical Engineering Journal*, 362, pp.1-10. [DOI]
- Zhang, L., Zhang, C., Hu, C. and Liu, H., 2021. Anaerobic treatment of municipal wastewater in high-altitude regions: challenges and adaptations. *Science of the Total Environment*, 754, pp.142156. [DOI]